A REMPI and ZEKE Spectroscopic Study of a Secondary Amide Group in Acetanilide

Susanne Ullrich and Klaus Müller-Dethlefs*

Department of Chemistry, The University of York, Heslington, York, YO10 5DD U.K.

Received: December 31, 2001; In Final Form: July 9, 2002

Vibrationally resolved REMPI and ZEKE spectra of acetanilide are presented with assignments based on CASSCF/cc-pVDZ ab initio calculations and symmetry considerations of different methyl rotor states. ZEKE spectra selectively recorded via intermediate rotor states of a particular symmetry allow us to directly measure the splittings of the $0a_1$ and 1e rotor levels in the S_0 state. Methyl group rotational features in the REMPI and ZEKE spectra are assigned from a simulation of methyl internal rotor levels in a one-dimensional model using a periodic V_3-V_6 potential, and barrier heights for methyl group rotation are extracted for the S_0, S_1, and D_0 states. Additional vibrational features corresponding to displacements of the amide group and side-chain are identified and analyzed by comparison to formanilide which was studied previously (Ullrich, S.; et al. *Phys. Chem. Chem. Phys.* **2001**, *3*, 5450; *Angew. Chem. Int. Ed.* **2002**, *41*, 166).

1. Introduction

The simplest *N*-phenylamide extensively studied in the neutral ground and excited state and very recently in the cationic state is formanilide and its hydrated clusters.[1−8] Both, the cis- and the trans[9] isomers of formanilide were observed in gas-phase molecular beam REMPI and ZEKE spectra, although the *cis*-formanilide was less abundant (6.5% and 94%, respectively).[1,10] This shows that *trans*-formanilide is more stable and conformationally favored in the neutral ground state.

Acetanilide, another *N*-phenylamide, is exclusively observed in a trans configuration in the gas phase[10] which is in agreement with the solid-phase structure as determined by X-ray[11] and neutron diffraction[12] studies. It adopts a C_s symmetry structure with all of the heavy atoms lying in the aromatic plane.[13] Two methyl hydrogen atoms are below and above the aromatic plane, and the third faces toward the amide group oxygen. A planar cis arrangement was found to be a transition state in B3LYP/6-31G* ab initio calculations by Caminati et al.,[13] which was attributed to the steric hindrance of the large methyl group. The global minimum energy structure of the cis isomer is twisted similar to formanilide, but additionally, a perpendicular cis structure was also found to be a local minimum.[13] However, the *cis*-acetanilide conformations are relatively higher in energy than the planar *trans*-acetanilide, explaining the failure to observe the cis form under supersonic jet cooled conditions where the population is quenched into the lowest energy conformation.[10]

This work on acetanilide is part of a series of studies on *N*-phenylamides. Although the neutral S_0 and S_1 states of these compounds and their water complexes have received considerable attention, the data on cationic amides is rather limited at present. Upon ionization, a significant amount of charge delocalizes from the aromatic ring to the side-chain, which justifies the use of these compounds as a cationic model system for a peptide bond. Whereas the amide group in formanilide is an end group attached to the aromatic ring, in acetanilide, the amide group takes a more central position because of the attachment of the methyl group. It allows the study of the peptidic bond modeled as a linkage between different molecular units. This paper presents a detailed spectroscopic and ab initio study of the acetanilide monomer. It is an important precursor for the following cluster studies,[14] where preferences in solvation sites and intermolecular interactions, but also the effect of solvation on the monomer (e.g., torsional potential, conformational choice, ...) will be explored.

2. Experimental and Computational Details

2.1. Experimental Techniques. Acetanilide (Aldrich, 97% purity) was heated to 140 °C in a sample reservoir located directly behind the valve and expanded in a supersonic jet through a 1 mm diameter nozzle using Ne as a backing gas at a stagnation pressure of 1−2 bar. The experimental apparatus and techniques have been described previously in detail and will only be summarized briefly here.[15] The molecular beam interacts with the frequency-doubled output of two excimer-pumped dye lasers. The ions from a REMPI process and ZEKE electrons are extracted in perpendicularly arranged ion and electron optics, with the ions additionally going through a reflectron. The same pulses were employed as in ref 15. All wavelengths were calibrated by simultaneously recording iodine absorption spectra as a reference and values have been converted from air to vacuum.

2.2. Simulations of Internal Methyl Rotor Levels. The progressions of methyl internal rotations in the REMPI and ZEKE spectra are analyzed using a V_3-V_6 potential in a one-dimensional rotor model as described, for example, in ref 22. The potential for internal rotation is expressed by (in this case up to $n = 2$)

$$V(\varphi) = \sum_n \frac{V_{3n}}{2}(1 - \cos(3n\varphi))$$

where φ would be the torsional angle between the methyl group and molecular plane. The Hamiltonian is given by

$$H = -B\frac{\partial^2}{\partial\varphi^2} + V(\varphi)$$

* To whom correspondence should be addressed. E-mail: kmd6@york.ac.uk. Fax: +44 1904 432516.

10.1021/jp014683w CCC: $22.00
Published on Web 09/13/2002

where B is the reduced internal rotational constant of the methyl rotor around the methyl top axis. A basis set of harmonic one-dimensional free rotor wave functions $\cos(m\varphi)$ and $\sin(m\varphi)$ is used to determine the eigenvalues of the Hamiltonian; m is the internal rotor quantum number. The parameters B, V_3, and V_6 are varied in the simulation until the observed methyl rotor states in the REMPI and ZEKE spectra fit the calculated eigenvalues best.[16]

The assignment of the spectra are based on the following procedures:

(1) The assignments of the methyl group internal rotations are obtained from the simulations described above.

(2) Visual inspection of partially rotationally resolved band contours is used as an additional verification of the symmetry of the transition. Features of a_1 symmetry show a "broadened", "split" band profile (b-type character), whereas e ↔ e transitions are narrower, "single peak" bands (c-type character, indicated by a prominent Q-branch).[17]

(3) Methyl rotor excitations should appear as transitions of a single symmetry $a_1 \leftrightarrow a_1$ and e ↔ e. Normal modes that are uncoupled from the methyl rotor should show both a_1 and e symmetry components with a splitting more or less identical to the origin band. Vibrations of totally symmetric transitions that are coupled to the methyl rotor will also display both symmetry components, although with a different splitting. Vibrational excitation can modify the methyl rotor potential leading to an averaged, effective potential, a change in barrier height and consequently a different methyl rotor level splitting.

(4) ZEKE spectra recorded via intermediate levels of a particular symmetry species provide additional confirmation for assignments of the REMPI spectrum.

2.3. Ab Initio Calculations. To complement the experimental work, ab initio calculations were performed at the CASSCF-(10/9,8)/cc-pVDZ level of theory for the S_0, S_1, and D_0 states with additional single-point CASMP2 energies. The active space consisted of the following HF orbitals: the six benzene type π orbitals and the oxygen and nitrogen lone pairs of a″ symmetry. This level of theory was successfully applied in our previous work on *trans*-formanilide.[1,2] In the geometry optimizations, only the experimentally observed trans isomer of acetanilide[10] was considered. Harmonic frequencies were determined to ensure optimized structures were local minima and to aid the assignment of the REMPI and ZEKE spectra. Mulliken, ESP, and NPA charges were computed. The latter had proven earlier to give reasonable results for charge delocalization in molecules with flexible side-chains.[24] All ab initio calculations were performed on an IBM RS/6000 using Gaussian 98.[25]

3. Results and Discussion

3.1. CASSCF ab Initio Calculations. The CASSCF geometry optimizations predict that *trans*-acetanilide adopts a planar, C_s, symmetry structure in all three states (S_0, S_1, and D_0) with two of the methyl hydrogens above and below the molecular plane and one methyl hydrogen facing the amide oxygen. An optimized ab initio geometric structure of *trans*-acetanilide is displayed in Figure 1 including geometric parameters in the S_0, S_1, and D_0 states at the CASSCF/cc-pVDZ level of theory. Full geometries are available as Supporting Information in Table A. The ground state planarity was confirmed by microwave absorption spectroscopy by Caminati et al.[13] showing excellent agreement between experimentally determined (A = 3776.614 MHz; B = 783.520 MHz; C = 649.666 MHz) and CASSCF (A = 3740.081 MHz; B = 780.321 MHz; C = 648.232 MHz) rotational constants.

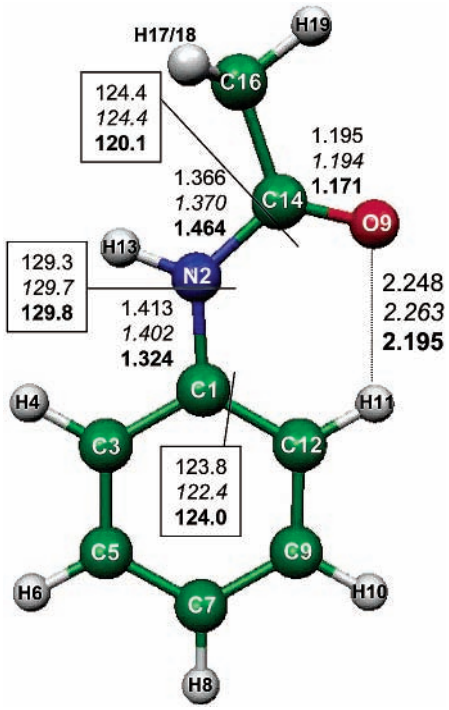

Figure 1. CASSCF/cc-pVDZ optimized geometry of *trans*-acetanilide including the labeling of atoms. Geometric parameters of the side chain are given for the S_0 (normal), S_1 (italic), and D_0 (bold) states.

Upon excitation, CASSCF calculations predict only minor changes in side-chain bond distances and angles. Changes in these geometric parameters become considerably more pronounced upon $D_0 \leftarrow S_1$ ionization. The C1−N2, C14−C16, and C14−O9 bond lengths shorten, whereas N2−C14 elongates. The bond angles C12−C1−N2 and C1−N2−C14 increase, but N2−C14−O9 decreases. The distance between the side-chain O9 and the ring H11 decreases. These geometry changes mainly correspond to an in-plane bend, B′, and stretch, Σ′, of the side-chain which are therefore expected to appear with moderate intensity in the REMPI and notable intensity in the ZEKE spectra.

Excitation and ionization energies are given in Table B (Supporting Information). Experimental excitation energies are reproduced within 2% at the CASSCF level of theory including MP2 and ZPE corrections. This is an excellent agreement considering the difficulties associated with excited-state calculations.[26] Ionization energies show an agreement within 0.4%. Harmonic frequencies are listed in Table C (Supporting Information) including labels based on Wilson notation.[27] Many ring modes show considerable side-chain displacements and labels can only be seen as a guide.

3.2. Determination of S_0 State $0a_1$−1e Methyl Rotor Level Splitting using ZEKE Spectroscopy. In the electronic ground state, both methyl rotor states of a and e symmetry are populated under supersonic jet conditions. All of the population is quenched into the rotor states of $0a_1$ and 1e symmetry and remains there, because a ↔ e transitions are nuclear spin forbidden. The lowest energy peak in all ZEKE spectra at around 65 537 cm^{-1} corresponds to the ionization energy. Slightly larger discrepancies in experimental ionization energies via different modes than usual (± 5 cm^{-1}) can be related to the ground-state splitting between $0a_1$ and 1e components selectively ionized via an intermediate state of a certain symmetry. For instance, the ionization energy in the ZEKE spectrum recorded via $CH3^1$ (2e) is slightly lower (see Table 2). In fact, ZEKE spectroscopy can be used to measure directly the a−e splitting in the ground-

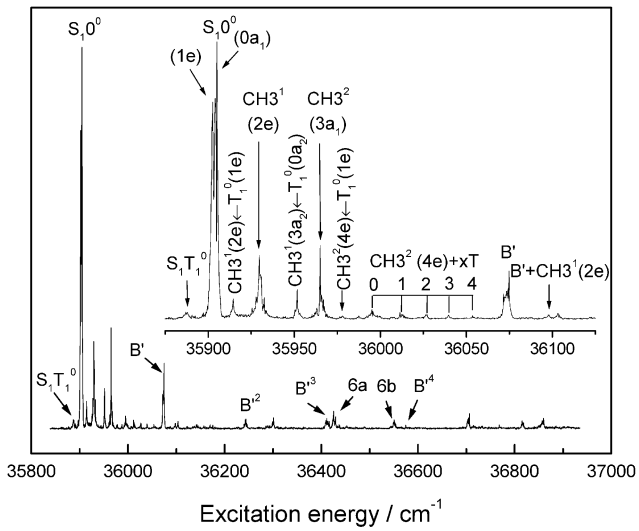

Figure 2. Two-color (1+1′) REMPI spectrum of *trans*-acetanilide recorded with the ionization laser set to 30075 cm^{-1}.

state S_0. Because $0a_1$ and 1e methyl rotor levels in the cation are degenerate (the barrier is too high to cause any appreciable spliiting), the difference in ionization energies of ZEKE spectra recorded via intermediate states of A and E symmetry directly resemble the ground-state splitting. For acetanilide, this is ∼4.5 ± 0.5 cm^{-1}. For the S_0 state, only the splitting of the lowest level into $0a_1$ and 1e components could be determined experimentally from the ZEKE spectra. Therefore, barrier heights obtained from the methyl rotor simulation can only be estimated very roughly to be around 10−30 cm^{-1}. However, this indicates that the barrier height is substantially below the value of 49.7 cm^{-1} given by Caminati et al.[13]

3.3. REMPI Spectrum of Acetanilide. The two-color (1+1′) REMPI spectrum of acetanilide with the ionization laser set to 30 075 cm^{-1} is shown in Figure 2. It is almost identical to the previously published (1+1) REMPI spectrum by Cable and coworkers[10] which was recorded in a He expansion. All peak positions are exactly reproduced, and relative intensities are in very good agreement.

The dominant S_1 0^0 origin peak and only limited intramolecular vibrational excitation suggests minor geometry changes upon excitation in line with the predictions from the CASSCF calculations. The fact that no dominant long, equally spaced progressions of the torsional and out-of-plane bending modes are observed as in the nonplanar *cis*-formanilide,[1,10] and *N*-methylformanilide[10] supports a planar structure of *trans*-acetanilide.

As can be seen in Figure 3a the S_1 0^0 band is clearly split into two components. The S_1 0^0 (1e) occurs at 35 902.4 ± 0.2 cm^{-1} and the S_1 0^0 ($0a_1$) at 35 904.7 ± 0.2 cm^{-1} which compares to an excitation energy of 36 663 cm^{-1} predicted by ab initio calculations at the CASMP2/cc-pVDZ level of theory including ZPE corrections. The S_1 state origin band is split by 2.3 ± 0.2 cm^{-1}, and the appearance of $0a_1$ and 1e internal methyl rotor symmetry species is reversed; that is, the 1e ← 1e transition appears at a lower energy than $0a_1$ ← $0a_1$. This can be extracted from the simulation of methyl rotor states that fit all levels best. It is also confirmed by comparison to the rotational band contours of the $CH3^1$ (2e) and $CH3^2$ ($3a_1$) peaks (Figures 3b and 3c), whose symmetry and identity is known from their ZEKE spectra. Combining the ground-state splitting obtained from ZEKE spectroscopy (see previous section) and the splitting of the S_1 0^0 transition leads to a splitting of 2.2 ± 0.5 cm^{-1}

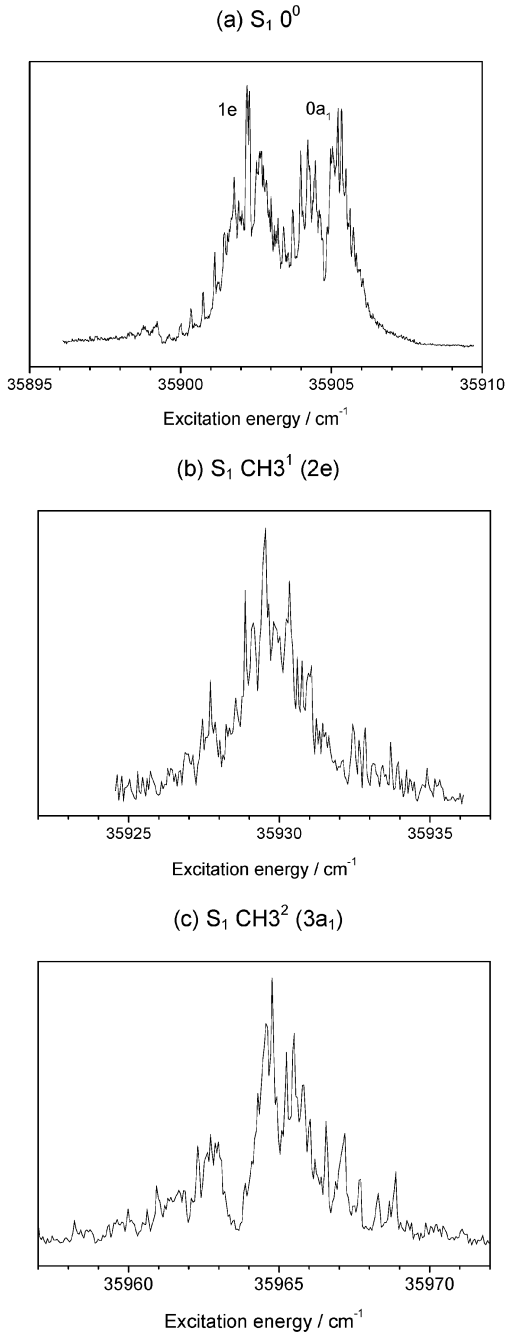

Figure 3. High-resolution REMPI spectra of (a) S_1 0^0(1e, $0a_1$), (b) S_1 $CH3^1$ (2e), and (c) S_1 $CH3^2$ ($3a_1$) of *trans*-acetanilide.

between the $0a_1$ and 1e levels in the excited S_1 state. The barrier height for methyl group internal rotation in the excited S_1 state can be determined relatively accurately from the simulation including all methyl rotor features observed in the REMPI spectrum. Its value is 52 ± 5 cm^{-1}; the barrier height for methyl group rotation is higher in the neutral excited state than in the ground state.

The vibrational features observed on the S_1 0^0 origin of *trans*-acetanilide can be mainly attributed to the low-frequency modes of the side chain. The very weak peak to the red of S_1 0^0 (−14 cm^{-1}) is a hot band that results from population of a vibrational level in the ground state. It can be assigned to the lowest frequency mode T, the C1−N2 torsion of the side-chain with respect to the phenyl ring, which is predicted by the CASSCF/cc-pVDZ calculation to occur at 25 cm^{-1} in the S_0 and at 27 cm^{-1} in the S_1 state.

A very similar vibrational pattern is observed on S_1 T_1^0 and S_1 0^0 that is attributed to excitation of methyl group rotation. The simulation of the methyl rotor levels in a finite V_3-V_6 periodic potential is presented together with the experimental values in Table 3. A progression of methyl group rotations is observed with $CH3^1$ (2e) appearing at 28 cm^{-1} above S_1 0^0 and the second quanta at $CH3^2$ ($3a_1$) at 61 cm^{-1} and $CH3^2$ (4e) at 93 cm^{-1}. The latter is followed by a progression of combination bands with up to four quanta of side chain torsional excitation, $CH3^2$ (4e) + T^1 to $CH3^2$ (4e) + T.[4] The $CH3^1$ (2e) and $CH3^2$ ($3a_1$) were used as intermediate resonances for ZEKE spectra and can therefore be assigned unambiguously. An analogous pattern of vibrational features is observed in the S_1 T_1^0 band. The methyl group rotation, $CH3^1$ (2e), is observed at 26 cm^{-1} and the overtone, $CH3^1$ ($3a_2$) and $CH3^2$ (4e), at 64 cm^{-1} and at 90 cm^{-1} above the S_1 T_1^0 band. A similar combination with a side chain torsional progression is possibly built on the peak at 90 cm^{-1} as very weak features in this frequency range indicate, however, covered by the more intense progression on the S_1 0^0 and not unambiguously identifiable. The assignment of the low-frequency features of the acetanilide REMPI spectrum to progressions and combination bands on two different origin peaks, the S_1 T_1^0 and S_1 0^0, is supported by the different peak shapes of the features belonging to each series with almost exactly matching frequency spacings. The torsional motion is coupled to the methyl group rotation, and consequently, levels are split into states of a_2 and e symmetry. Transitions occur according to G_6 selection rules, with $a_2 \leftrightarrow a_2$ and $e \leftrightarrow e$ transitions being allowed.[33]

Alternatively, the feature at 12 cm^{-1} above the S_1 0^0 (1e) origin could be assigned to a T_0^1 transition and the peak at 50 cm^{-1} to the out-of-plane bend B_N of the side-chain, predicted to appear at 27 and 83 cm^{-1} by the S_1 state CASSCF calculation, respectively. Both out-of-plane modes show a coupling to the methyl rotation in the normal-mode analysis, which justifies their appearance in the REMPI spectrum as $e \leftrightarrow e$ transitions. This alternative assignment is supported by a later study of the acetanilide·H_2O complex,[14] where the peak at 12 cm^{-1} above S_1 0^0 (1e) was also observed at an almost identical frequency, but no side-chain torsional hot-band was present.

The peak of medium intensity at 167 cm^{-1} above the S_1 0^0 band can be assigned with certainty to the in-plane bending mode, B′, of the side-chain. It shows a similar broadening and structure as the origin peak and appears at a similar frequency as in *trans*-formanilide (196 cm^{-1}) which is in good agreement with the ab initio predictions. Additionally, the ZEKE spectrum recorded via this mode (Figure 4d) strongly supports this assignment. The in-plane bend, B′, shows a progression of possibly up to four quanta indicative of the side chain geometry changes predicted by the ab initio calculations. The anharmonicity of this vibration was assessed using a Morse potential,[28] which provided $\omega_e = 103$ cm^{-1} and $\omega_e\chi_e = 12.5$ cm^{-1}.

In the higher frequency region of the spectrum at 522 and 647 cm^{-1}, ring modes, possibly 6b and 6a, including significant contributions in side-chain displacements, are observed. This assignment is based on the ab initio results and comparison to *trans*-formanilide.[2]

All vibrational features evident in the REMPI spectrum are listed in Table 1 together with the suggested assignments and the CASSCF harmonic frequencies.

3.4. ZEKE Spectra of Acetanilide. The ZEKE spectra recorded via different S_1 intermediate states are presented in Figure 4 and vibrational features and their assignment together with CASSCF/cc-pVDZ harmonic frequencies are summarized in Table 2. Experimental and simulated methyl rotor frequencies are shown in Table 3. The barrier height for methyl group rotation is highest in the cationic state as the observed splitting between methyl rotor states of different symmetries suggest. Although the ionization energy peak and $CH3^1$ (2e, $3a_2$) are still not significantly split, the $CH3^2$ ($3a_1$) and $CH3^2$ (4e) states show a splitting of 5 cm^{-1} that increases for $CH3^3$ (5e) and $CH3^3$ ($6a_2$) to 12 cm^{-1}. It should be noted that $a_2 \leftrightarrow a_1$ transitions are observed in the ZEKE spectra albeit only with small intensity. This is another observation in line with earlier observations of symmetry forbidden transitions in ZEKE spectra.[29] The deeper reasons for this are still under study.

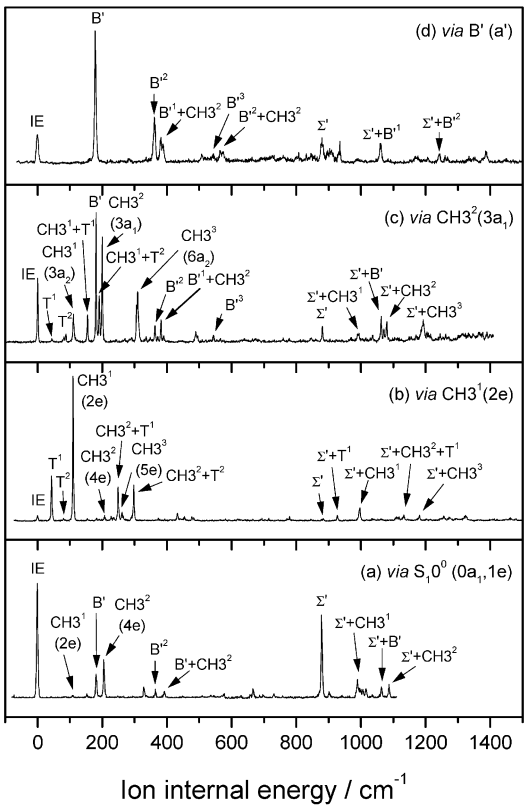

Figure 4. ZEKE spectra of acetanilide recorded via (a) the S_1 0^0, the methyl group rotations (b) $CH3^1$(2e) and (c) $CH3^2$($3a_1$), and (d) the side-chain in-plane bend B′. All spectra are displayed relative to the ionization energy of *trans*-acetanilide from either the S_0 0^0 state of $0a_1$ or 1e symmetry. Exact ionization energies are included in Table 3.

Figure 4a shows the ZEKE spectrum via the S_1 0^0 band. In addition to a dominant ionization energy peak the in-plane bend, B′, and overtone of the methyl rotation, $CH3^2$ (4e) appears with medium intensity. A very weak peak at 109 cm^{-1} can be assigned to $CH3^1$ of 2e symmetry. The appearance of different symmetries in the ZEKE spectrum recorded via the S_1 origin can be attributed to the partial overlap of both components, $0a_1$ and 1e, in the S_1 0^0 band and excitation of both contributions.

TABLE 1: Vibrational Features Observed in the (1+1′) REMPI Spectrum of *trans*-Acetanilide Together with Assignments and CASSCF/cc-pVDZ Harmonic Frequencies of the S_1 State[a]

	rel. position			rel. position		
peak position	to 35902 cm^{-1}	to 35904 cm^{-1}	assignment	to 35888 cm^{-1}	assignment	CASSCF
35888 vw	(−14)	(−16)		0	T_1^0	25[b]
35902 vs	0	−2	$S_1\ 0^0$ (1e)			
35904 vs	(2)	0	$S_1\ 0^0$ ($0a_1$)			
35905 vs	(3)	1				
35914 w	(12)	(10)		26	S_1CH3^1 (2e) ← S_0T_1	
35930 m	28	(26)	$CH3^1$ (2e)			47
35952 w	(50)	(48)		64	S_1CH3^2 ($3a_2$) ← S_0T_1	
35965 m	(63)	61	$CH3^2$ ($3a_1$)			
35978 vvw	76	74		90	$S_1\ CH3^2$ (4e) ← S_0T_1	
35987 vvw	85	83				
35995 vw	93	(91)	$CH3^2$ (4e)	107[c]	$S_1\ CH3^2$ (4e) + T^1 ← S_0T_1	
36012 vw	110	(108)	$CH3^2$ (4e)+T^1	124[c]	$S_1\ CH3^2$ (4e) + T^2 ← S_0T_1	
36027 vw	125	(123)	$CH3^2$ (4e)+T^2	139[c]	$S_1\ CH3^2$ (4e) + T^3 ← S_0T_1	
36040 vw	138	(136)	$CH3^2$ (4e)+T^3	152[c]	$S_1\ CH3^2$ (4e) + T^4 ← S_0T_1	
36054 vw	152	(150)	$CH3^2$ (4e)+T^4			
36071 m	169	167	B′			181
36098 vw	196	194	B′$CH3^1$ (2e)			
36103 vw	201	199				
36244 w	342	340	B'^2			
36301 w	399	397				
36411 vw	509	507	B'^3			
36426 vw	524	522	6b			582
36551 vw	649	647	6a (?)			699
36575 vvw	673	671	B'^4			
36706 vw	804	802				
36817 vw	915	913				
36860 vw	958	956				

[a] All frequencies are given in cm^{-1} with an absolute error of ±0.2 cm^{-1}. Intensities are denoted as vvw = very very weak, *vw* = very weak, w = weak, m = medium, s = strong, and vs = very strong. [b] From S_0 state CASSCF calculation. [c] If observable, progressions and combination bands on the $S_1T_1^0$ origin would be hidden under the more intense S_10^0 features.

The overtone of the in-plane bend, B′, and the combination band B′ + $CH3^2$ can be identified. All vibrations are observed again on the side-chain stretch, Σ′, which is also very pronounced in this spectrum.

The ZEKE spectrum recorded via $S_1\ CH3^1$ (2e) is displayed in Figure 4b. The band origin appears weakly because of poor Franck−Condon overlap. Compared to the ZEKE spectrum obtained via the $S_1\ 0^0$, all out-of plane modes, such as the torsion and the CH_3 rotation, are significantly enhanced in their first and third quanta but relatively weak as even quanta explainable again by Franck−Condon overlap of methyl rotor eigenfunctions in the S_1 and D_0 state. The most intense transition is to the $CH3^1$ (2e) vibration in line with strong $\Delta v = 0$ propensity and symmetry considerations. Again, the vibrational features are repeated on the side-chain stretch Σ′.

The ZEKE spectrum recorded through the intermediate $CH3^2$ ($3a_1$) is presented in Figure 4c. Compared to the previous spectrum vibrational features extend to higher frequencies as progressions or combination bands, the in-plane bend B′, which did not appear in the ZEKE spectrum via $CH3^1$ (2e) due to small Franck−Condon factors, is now the most intense feature together with the second quantum of the methyl rotation $CH3^2$ ($3a_1$). Representing the geometry changes upon ionization, the in-plane bend, B′, shows a progression of up to three quanta and a combination band with the $CH3^2$ internal rotation. All peaks appear again built on the side-chain stretch, Σ′.

The ZEKE spectrum via the S_1 B′ band (Figure 4d) is considerably less crowded than the two spectra recorded via intermediate methyl rotor modes. Vibrational features in this spectrum can be assigned with certainty. The most prominent peak is the in-plane bend, B′, which would be expected to be of very strong intensity from the anticipated $\Delta v = 0$ propensity. The mode shows a long progression of up to 3 quanta which is in line with the geometry changes along these coordinates predicted by the CASSCF calculations upon ionization. The progression is repeated again on the side-chain stretch Σ′. The relatively low intensity of the ionization energy peak can be attributed to Franck−Condon factors. From the progressions of the in-plane side-chain bend, B′, observed in the different ZEKE spectra, ω_e and $\omega_e\chi_e$ can be estimated to be 96 and 18.4 cm^{-1}, respectively.

4. Conclusions

This work is part of a series of studies on *N*-phenylamides. Characteristic similarities are observed in the REMPI and ZEKE spectra of the trans isomers of formanilide and acetanilide which demonstrate the flexibility and geometry changes of the side-chain/amide group upon excitation and ionization. In summary, the spectra of acetanilide, where the peptide bond assumes a more centered position than in formanilide, show a decrease in vibrational frequencies of intramolecular modes, e.g., side-chain bend B′ and stretch Σ′. In acetanilide, the oxygen lone pair electron density can additionally delocalize onto the C14−CH_3 bond, which might weaken the conjugation toward the ring. The result would be a decrease in vibrational frequencies centered on the N2−C14 bond. Additionally, methyl rotor features in acetanilide have been assigned in the REMPI and ZEKE spectra and barrier heights estimated for the S_0, S_1, and D_0 states as 10−30, 52, and 325 cm^{-1}, respectively. Previously published work on anisole and dimethoxybenzenes[30] showed torsional excitation of the whole methoxy group but no explicit methyl rotor excitation. Similarly, in our earlier work on 3-methoxyphenol,[31] no prominent features related to methyl group rotation were observed in the low frequency region of the REMPI and ZEKE spectra. The pronounced observation of methyl group rotation in acetanilide was consequently somewhat unexpected

TABLE 2: Vibrational Features in cm^{-1} Observed in the ZEKE Spectra of *trans*-Acetanilide Recorded via (a) S_1 0^0, (b) $CH3^1$ (2e), (c) $CH3^2$ ($3a_1$), and (d) B′[a]

relative position					
(a) via S_1 0^0	(b) via S_1 $CH3^1$ (2e)	(c) via S_1 $CH3^2$ ($3a_1$)	(d) via S_1 B′	CASSCF	assignment
0 vs	0 w	0 m	0 w		IE
(65536 ± 5 cm^{-1})	(65535 ± 5 cm^{-1})	(65540 ± 5 cm^{-1})	(65539 ± 5 cm^{-1})		
	43 m	44 vw		48	T^1
	78 vw	88 vw			T^2
109 vw	110 vs	111 w		138	$CH3^1$ (2e,$3a_2$)
152 vw	154 vw	155 w			$CH3^1$ (2e,$3a_2$) + T^1
181 m	182 vw	181 s	178 s	192	B′
		190 m			$CH3^1$ ($3a_2$) + T^2
		200 s			$CH3^2$ ($3a_1$)
205 m	208 vw				$CH3^2$ (4e)
	227 vw				T^5 (?)
	235 vw				
	249 m				$CH3^2$ (4e) + T^1
	261 w				$CH3^3$ (5e)
	297 m				$CH3^2$ (4e) +T^2
		309 m			$CH3^3$ ($6a_2$)
329 w					B′ + $CH3^1$ (2e) +T^1 (?)
364 w		362 w	361 m		B'^2
		382 w	381 w		B′ + $CH3^2$ ($3a_1$)
392 w		390 vw	388 w		B′ + $CH3^2$ (4e)
	433 w				$CH3^2$+T^5 (?)
	454 vw				
	477 vw				
		490 w			
			507 vw		
		542 w	545 vw		B'^3
			565 vw		B'^2+$CH3^2$
577 vw			575 vw		
666 w					
878 s	884 vw	880 vw	880 w	944	Σ′
901 vw			903 vw		
	927 w		935 w		Σ′+T^1
990 w	997 w	991 vw			Σ′+$CH3^1$ (2e, $3a_2$)
1062 w		1063 w	1061 w		Σ′+B′
		1071 vw			
1087 w		1081 w			Σ′+$CH3^2$ ($3a_1$)
	1133 vw				Σ′+$CH3^2$ (4e) + T^1
	1181 vw	1192 w			Σ′+$CH3^3$ ($6a_2$)
			1242 vw		Σ′+B'^2
	1257 vw				
	1272 vw				
	1324 vw				
			1388 vw		

[a] Intensities are given as vvw = very very weak, vw = very weak, w = weak, m = medium, *and* s = Strong. Assignments and CASSCF/cc-pVDZ harmonic frequencies of the D_0 state are also presented.

TABLE 3: Experimentally Determined Methyl Rotor States of *trans*-Acetanilide in the S_0, S_1, and D_0 States Compared to Simulated Eigenvalues[a]

assignment	experimental/cm^{-1}	simulated/cm^{-1}
S_0 state		B=5.2, V_3= 10−30,V_6=−20
$0a_1$	0	0
1e	5	5
S_1 state		B=5.2, V_3=52, V_6=−20
$0a_1$	0	0
1e	2	3
2e	30	30
$3a_1$	61	62
4e	95	91
D_0 state		B=5.2, V_3=325, V_6=0
$0a_1$	0	0
1e	0	0
2e	110	110
$3a_1$	200	199
4e	208	206
5e	261	267

[a] All frequencies are given relative to $0A_1$ level of the corresponding state.

but might be explained by a considerably less rigid structure of the −C−CH_3 in acetanilide than −O−CH_3, which might have some double bond character.

The work presented in this paper could benefit from further experiments to allow a more definite assignment and interpretation of the REMPI spectrum. For example, additional ZEKE spectra selectively recorded via different symmetry components of split features and hole-burning experiments together with deuteration experiments could resolve some of the ambiguities. However, this was considered beyond the scope of this study, which was aimed to investigate the spectroscopy of the amide bond, particularly in the cationic state.

The use of acetanilide as a further model peptide can be justified from the ab initio calculations for the following reasons: Acetanilide adopts a planar amide bond structure in the commonly observed *trans* arrangement. The normal-mode analyses in the frequency calculation shows that some vibrational features observed in the spectra can be attributed to vibrations with displacements mainly localized on the amide group. Furthermore, ab initio calculations suggest that, in contrast to formanilide, in acetanilide the low-frequency torsion in the cation corresponds to a twisting motion around the NH−CO amide bond, although, in the neutral, it still corresponds to the C1−N2 torsion. The normal-mode analysis of the torsion is supported by the elongation in N2−C14 but shortening of the C1−N2 bond lengths in the cation. Mulliken, ESP, and NPA

charges calculated at the CASSCF/cc-pVDZ level of theory are available as Supporting Information Table D. All different methods predict a charge delocalization of around 40% onto the side-chain (and 32% onto the amide group itself). This compares to about 39% (and 32%) in formanilide.[32] Concluding, acetanilide can be seen as a good model system for a cationic peptide bond, although the nearly freely rotating methyl group adds complication to the spectral analysis. However, because of coupling between some vibrations and the methyl group rotation, transitions to out-of-plane modes can become allowed in the G_6 molecular symmetry group[33] and gain considerable intensity. Torsional potentials of the side chain/amide group, which had been shown to be the key process in long-range charge transfer in polypeptides,[34] become accessible by REMPI and ZEKE spectroscopy. In previous work, we tried to use complexation with an Ar atom to break the C_s symmetry of formanilide; however, we failed to observe torsional features with notable intensity.[3] Additionally, the pronounced occurrence of methyl rotation throughout the spectra demonstrates clearly that excitation is not restricted to the aromatic chromophore but partially occurs on the side chain as anticipated.

These relatively small peptide model systems serve as important precursors for the investigation of more flexible and larger biomolecules in the gas phase. The attachment of the methyl group made this study significantly more challenging than formanilide. Precursor studies of the type presented here will aid to characterize and analyze more complex systems. Molecular systems that would be of interest to extend this work on model peptides are, for example, cationic *N*-benzylformamide,[35] which includes a CH_2 spacer between the ring and the amide group that could minimize artifacts due to ring attachment. CH_2 is also a very common neighbor to amide groups in peptides and proteins. To center the amide group more as a linkage element between different molecular units, replacement of the methyl group with longer chains or even attachment of a second peptide group would be of interest.

Acknowledgment. We thank the Engineering and Physical Sciences Research Council (EPSRC, Grant GR/M48451) for financial support. The authors thank Xin Tong for his help at the experiment. We are most grateful to Masaaki Fujii (Okazaki) for providing us with his internal rotor fitting program. S.U. acknowledges support from the Fonds des Verbandes der Chemischen Industrie followed by a DAAD Doktorandenstipendium im Rahmen des gemeinsamen Hochschulsonderprogramms III von Bund und Ländern.

Supporting Information Available: Full geometries (Table A), excitation and ionization energies (Table B), harmonic frequencies (Table C), and Mulliken, ESP, and NPA charges calculated at the CASSCF/cc-pVDZ level of theory (Table D). This material is available free of charge at http://pubs.acs.org.

References and Notes

(1) Ullrich, S.; Tarczay, G.; Tong, X.; Dessent, C. E. H.; Müller-Dethlefs, K. *Angew. Chem., Int. Ed.* **2002**, *41*, 166.

(2) Ullrich, S.; Tarczay, G.; Tong, X.; Dessent, C. E. H.; Müller-Dethlefs, K. *Phys. Chem. Chem. Phys.* **2001**, *3*, 5450.

(3) Ullrich, S.; Tarczay, G.; Tong, X.; Ford, M. S.; Dessent, C. E. H.; Müller-Dethlefs, K. *Chem. Phys. Lett.* **2002**, *351*, 121.

(4) Dickinson, J. A.; Hockridge, M. R.; Robertson, E. G.; Simons, J. P. *J. Phys. Chem. A* **1999**, *103*, 6938.

(5) Fedorov, A. V.; Cable, J. R. *J. Phys. Chem. A* **2000**, *104*, 4943.

(6) Mons, M.; Dimicoli, I.; Tardivel, B.; Piuzzi, F.; Robertson, E. G.; Simons, J. P. *J. Phys. Chem. A* **2000**, *105*, 969.

(7) Robertson, E. G. *Chem. Phys. Lett.* **2000**, *325*, 299.

(8) Ilieva, S.; Hadjieva, B.; Galabov, B. *J. Mol. Struct.* **1999**, *508*, 73.

(9) In line with the literature referenced within this paper, we have used cis and trans, although the correct notation would be syn and anti, respectively.

(10) Manea, V. P.; Wilson, K. J.; Cable, J. R. *J. Am. Chem. Soc.* **1997**, *119*, 2033.

(11) Wasserman, H. J.; Ryan, R. R.; Layne, S. P. *Acta Crystallogr. Sec. C* **1985**, *41*, 783.

(12) Johnson, S. W.; Eckert, J.; Barthes, M.; McMullan, R. K.; Muller, M. *J. Phys. Chem.* **1995**, *99*, 16253.

(13) Caminati, W.; Maris, A.; Millemaggi, A. *New J. Chem.* **2000**, *24*, 821.

(14) Ullrich, S.; Müller-Dethlefs, K. *J. Phys. Chem. A* **2002**, *106*, 9188.

(15) Haines, S. R.; Geppert, W. D.; Chapman, D. M.; Watkins, M.; Dessent, C. E. H.; Cockett, M. C. R.; Müller-Dethlefs, K. *J. Chem. Phys.* **1998**, *109*, 9249.

(16) The program used for the simulation of the methyl rotor eigenvalues was written by Dr. Ken Takazawa based on the paper of Lewis, J. P.; Laane, J. *J. Mol. Struct.* **1972**, *12*, 427. Prof. M. Fujii's (Institute for Molecular Sciences, Okazaki) assistance is gratefully acknowledged.

(17) Ford, M. S.; Haines, S. R.; Pugliesi, I.; Dessent, C. E. H.; Müller-Dethlefs, K. *J. Electron Spectrosc.* **2000**, *112*, 231.

(18) Held, A.; Selzle, H. L.; Schlag, E. W. *J. Phys. Chem. A* **1998**, *102*, 9625.

(19) Lu, K.-T.; Weinhold, F.; Weisshaar, J. C. *J. Chem. Phys.* **1995** *102*, 6787.

(20) Okuyama, K.; Mikami, N.; Ito, M. *J. Phys. Chem.* **1985**, *89*, 5617.

(21) Takazawa, K.; Fujii, M.; Ito, M. *J. Chem. Phys.* **1993**, *99*, 3205.

(22) Suzuki, K.; Emura, Y.; Ishiuchi, S.-I.; Fujii, M. *J. Electron Spectrosc.* **2000**, *108*, 13.

(23) Nakai, H.; Kawai, M. *Chem. Phys. Lett.* **1999**, *307*, 272.

(24) Patey, M. D.; Dessent, C. E. H. *J. Phys. Chem A* **2002**, *106*, 4623.

(25) Frisch, M. J.; Trucks, G. W.; Schlegel, H. B.; Scuseria, G. E.; Robb, M. A.; Cheeseman, J. R.; Zakrzewski, V. G.; Montgomery, J. A., Jr.; Stratmann, R. E.; Burant, J. C.; Dapprich, S.; Millam, J. M.; Daniels, A. D.; Kudin, K. N.; Strain, M. C.; Farkas, O.; Tomasi, J.; Barone, V.; Cossi, M.; Cammi, R.; Mennucci, B.; Pomelli, C.; Adamo, C.; Clifford, S.; Ochterski, J.; Petersson, G. A.; Ayala, P. Y.; Cui, Q.; Morokuma, K.; Malick, D. K.; Rabuck, A. D.; Raghavachari, K.; Foresman, J. B.; Cioslowski, J.; Ortiz, J. V.; Stefanov, B. B.; Liu, G.; Liashenko, A.; Piskorz, P.; Komaromi, I.; Gomperts, R.; Martin, R. L.; Fox, D. J.; Keith, T.; Al-Laham, M. A.; Peng, C. Y.; Nanayakkara, A.; Gonzalez, C.; Challacombe, M.; Gill, P. M. W.; Johnson, B. G.; Chen, W.; Wong, M. W.; Andres, J. L.; Head-Gordon, M.; Replogle, E. S.; Pople, J. A. *Gaussian 98*, revision A.7; Gaussian, Inc.: Pittsburgh, PA, 1998.

(26) Ullrich, S.; Müller-Dethlefs, K.; Knowles, P. J. *Phys. Chem. Chem. Phys.* To be submitted.

(27) Wilson, E. B. *Phys. Rev.* **1934**, *45*, 706.

(28) Atkins, P. W.; Friedman, R. S. *Molecular Quantum Mechanics*, 3rd ed.; Oxford University Press: New York, 1997.

(29) Müller-Dethlefs, K.; Schlag, E. W. *Angew. Chem., Int. Ed.* **1998**, *37*, 1347.

(30) Breen, P. J.; Bernstein, E. R.; Secor, H. V.; Seeman, J. L. *J. Am. Chem. Soc.* **1989**, *111*, 1958.

(31) Ullrich, S.; Geppert, W. D.; Dessent, C. E. H.; Müller-Dethlefs, K. *J. Phys. Chem. A* **2000**, *104*, 11864.

(32) CASSCF/cc-pVDZ NPA charges for the formanilide chain are in the S_0 state N7 = −0.74552, H1 = 0.40004, C7 = 0.73922, O1 = −0.70725, and H7 = 0.11149 and in the D_0 state: N7 = −0.60021, H1 = 0.43574, C7 = 0.72873, O1 = −0.56028, and H7 = 0.16712.

(33) Bunker, P. R.; Jensen, P. *Molecular Symmetry and Spectroscopy*, 2nd ed.; NRC Research Press: Ottawa, Canada, 1998.

(34) Schlag, E. W.; Sheu, S. Y.; Yang, D. Y.; Selze, H. L.; Lin, S. H. *Proc. Natl. Acad. Sci.* **2000**, *97*, 1068.

(35) Robertson, E. G.; Hockridge, M. R.; Jelfs, P. D.; Simons, J. P. *J. Phys. Chem. A* **2000**, *104*, 11714.